J|A|C|S ARTICLES

Published on Web 09/21/2009

Mimics of the Self-Assembling Chlorosomal Bacteriochlorophylls: Regio- and Stereoselective Synthesis and Stereoanalysis of Acyl(1-hydroxyalkyl)porphyrins

Teodor Silviu Balaban,[*,†,§,⊥] Anil Dnyanoba Bhise,[†] Gerhard Bringmann,[*,#] Jochen Bürck,[‡] Cyril Chappaz-Gillot,[⊥] Andreas Eichhöfer,[†] Dieter Fenske,[†,§,||] Daniel C. G Götz,[#] Michael Knauer,[#] Tadashi Mizoguchi,[▽] Dennis Mössinger,[†] Harald Rösner,[†] Christian Roussel,[*,⊥] Michaela Schraut,[#] Hitoshi Tamiaki,[*,▽] and Nicolas Vanthuyne[⊥]

Institute for Nanotechnology and Institute of Biological Interfaces, Forschungszentrum Karlsruhe, Karlsruhe Institute of Technology, Postfach 3640, D-76021 Karlsruhe, Germany, Center for Functional Nanostructures and Institut für Anorganische Chemie, Karlsruhe Institute of Technology, Universität Karlsruhe, D-76131 Karlsruhe, Germany, ISM2-Chirosciences, Faculté des Sciences, Université Paul Cézanne Aix-Marseille III, UMR 6263, Saint-Jérôme Case A62, Avenue Escadrille Normandie-Niemen, F-13397 Marseille, Cedex 20, France, Institute of Organic Chemistry and Röntgen Research Center for Complex Material Systems, University of Würzburg, Am Hubland, D-97074 Würzburg, Germany, and Department of Biosciences and Biotechnology, Faculty of Science and Engineering, Ritsumeikan University, Kusatsu, Shiga 525-8577, Japan

Received July 16, 2009; E-mail: silviu.balaban@int.fzk.de; bringman@chemie.uni-wuerzburg.de; christian.roussel@univ-cezanne.fr; tamiaki@se.ritsumei.ac.jp

Abstract: Diacylation of copper 10,20-bis(3,5-di-*tert*-butylphenylporphyrin) using Friedel−Crafts conditions at short reaction times, high concentrations of catalyst, and 0−4 °C affords only the 3,17-diacyl-substituted porphyrins, out of the 12 possible regioisomers. At longer reaction times and higher temperatures, the 3,13-diacyl compounds are also formed, and the two isomers can be conveniently separated by normal chromatographic techniques. Monoreduction of these diketones affords in good yields the corresponding acyl(1-hydroxyalkyl)porphyrins, which after zinc metalation are mimics of the natural chlorosomal bacteriochlorophyll (*BChl*) *d*. Racemate resolution by HPLC on a variety of chiral columns was achieved and further optimized, thus permitting easy access to enantiopure porphyrins. Enantioselective reductions proved to be less effective in this respect, giving moderate yields and only 79% ee in the best case. The absolute configuration of the 3^1-stereocenter was assigned by independent chemical and spectroscopic methods. Self-assembly of a variety of these zinc *BChl d* mimics proves that a collinear arrangement of the hydroxyalkyl substituent with the zinc atom and the carbonyl substituent is not a stringent requirement, since both the 3,13 and the 3,17 regioisomers self-assemble readily as the racemates. Interestingly, the separated enantiomers self-assemble less readily, as judged by absorption, fluorescence, and transmission electron microscopy studies. Circular dichroism spectra of the self-assemblies show intense Cotton effects, which are mirror-images for the two 3^1-enantiomers, proving that the supramolecular chirality is dependent on the configuration at the 3^1-stereocenter. Upon disruption of these self-assemblies with methanol, which competes with zinc ligation, only very weak monomeric Cotton effects are present. The favored heterochiral self-assembly process may also be encountered for the natural *BChl*s. This touches upon the long-standing problem of why both 3^1-epimers are encountered in *BChl*s in ratios that vary with the illumination and culturing conditions.

Introduction

Light-harvesting is the primary event in photosynthesis and certainly accounts for the vast majority of natural photosynthetic pigments such as carotenoids and chlorophylls (*Chl*s) in plants or bacteriochlorophylls (*BChl*s) in bacteria.[1] Life on Earth relies on photosynthesis either directly through photosynthetic organisms or through their incorporation into intricate food chains. Of course, all fossil fuels mankind presently consumes are also photosynthetic byproducts.[2,3] Because of different habitats, photosynthetic organisms have developed tailored light-harvesting (also called antenna) systems adapted to their specific environments. Thus, plants differ slightly in their light-harvesting ability from algae living at the water surface, all of which have *Chl*−protein complexes, which, in turn, differ from purple photosynthetic bacteria. In the past decade, some of these protein complexes have been structurally elucidated to atomic resolution

[†] Institute for Nanotechnology (INT), Karlsruhe Institute of Technology.
[‡] Institute of Biological Interfaces (IBG-2), Karlsruhe Institute of Technology.
[§] Center for Functional Nanostructures (CFN), Universität Karlsruhe (TH).
[||] Institut für Anorganische Chemie, Karlsruhe Institute of Technology, Universität Karlsruhe (TH).
[⊥] ISM2-Chirosciences, Université Paul Cézanne Aix-Marseille III.
[#] Institute of Organic Chemistry and Röntgen Research Center for Complex Material Systems, University of Würzburg.
[▽] Department of Biosciences and Biotechnology, Ritsumeikan University.

 10.1021/ja905628h CCC: $40.75

thanks to fascinating single-crystal X-ray studies.[4] Additionally, nanoscopic techniques applied to photosynthetic membranes have revealed spectacular nanostructures.[5]

There exist also green photosynthetic bacteria that can thrive in much deeper waters.[1,6] These organisms evolved some 2.5 billion years ago in an oxygen-free atmosphere. For light-harvesting, they have developed a curious organelle, the so-called *chlorosome*, or "green sac", which agglomerates *BChl*s *c*, *d*, and *e* (Chart 1). The chlorosomal architecture is based on self-assembly and not on proteins binding *BChl*s in specific sites.[7] No single-crystal X-ray diffraction data have yet been obtained from native chlorosomes, various mutants, or isolated *BChl*s, leaving room for much discussion on the exact nature of the supramolecular interactions. Bacteria expressing chlorosomes are real photon scavengers and use near-infrared radiation for light-harvesting. Once a stray photon is captured, its energy gets trapped by rapid energy-transfer steps with near-unity quantum efficiency in a *BChl*−protein complex, the so-called Fenna−Matthews−Olson (FMO) complex, which is attached to the baseplate of the chlorosome. The FMO complex actually was the very first (*B*)*Chl*−protein complex to be crystallized,[8] and its structure was solved by X-ray crystallography.[9] From the FMO complex, light energy is passed to the special pair of *BChl*s located in the nearby reaction center, where charge separation occurs. The uniqueness of the chlorosome as an antenna lies in the high chromophore density achieved by self-assembly. Usually, with nonspecific aggregated pigments, concentration quenching occurs which impairs the light-harvesting ability.

We have been interested in mimicking the self-assembly algorithm programmed into the *BChl c*, *d*, and *e* molecules with fully synthetic pigments such as porphyrins, chlorins, and, more recently, phthalocyanines.[10] By inducing chromophores to self-assemble, large functional nanostructures can be accessed without the need to meticulously assemble a covalent scaffold

Chart 1. (Left) Chlorosomal *BChl*s and Their Atom Numbering[a] and (Right) Schematic Representation of Our Synthetic Mimics Which Self-Assemble[b]

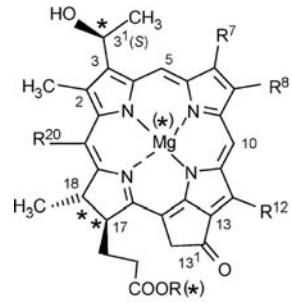

BChl *c* : $R^7 = CH_3$; $R^{20} = CH_3$
BChl *d* : $R^7 = CH_3$; $R^{20} = H$
BChl *e* : $R^7 = CHO$; $R^{20} = CH_3$

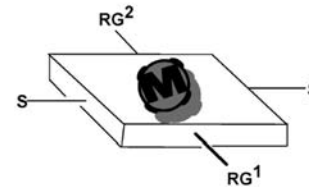

[a] The fatty alcohol (R−OH) esterifying the 17-propionic acid residue is farnesol in *Chlorobium* species which have a mixture of homologues differing in R^8 (Et, *n*-Pr, *i*-Bu) and/or R^{12} (Me, Et); *BChl c* from *Chloroflexus aurantiacus* has R^8 = Et and R^{12} = Me, with various R groups derived from phytol, stearol, cetol, geranyl-geraniol, etc. The formula shows the (3^1S)-configuration, but both epimers are present in varying amounts, which depend not only on the species but also on the culturing and illumination conditions applied. [b] M is a central metal atom, S are solubilizing groups such as long alkyl chains or 3,5-di-*tert*-butylphenyl residues, and RG^1 and RG^2 are recognition groups, which may be identical or different and are capable of ligating the central metal atom of adjacent molecules.[10e]

(1) (a) Blankenship R. E. *Molecular Mechanisms of Photosynthesis*; Blackwell: Oxford, 2002. (b) Balaban, T. S.; Tamiaki, H.; Holzwarth, A. R. In *Supramolecular Dye Chemistry*; Würthner, F., Ed.; Topics in Current Chemistry *258*; Springer Verlag: Berlin, 2005; pp 1−38. (c) Balaban, T. S. Light-harvesting Nanostructures. In *Encyclopedia of Nanoscience and Nanotechnology*; Nalwa, H. S., Ed.; American Scientific Publishers: Los Angeles, 2004; Vol. 4, pp 505−559.
(2) (a) Basic Research Needs for Solar Energy Utilization DOE Report, September 2005; www.sc.doe.gov/bes/reports/files/SEU_rpt.pdf. (b) Crabtree, G. W.; Lewis, N. S. *Physics Today* **2007**, *March*, 37–42.
(3) Balzani, V.; Credi, A.; Venturi, M. *Chem.−Eur. J.* **2008**, *14*, 26–39.
(4) (a) The LH2 of the purple bacteria *Rhodopseudomonas acidophila* at 2.5 Å resolution McDermott, G.; Prince, S. M.; Freer, A. A.; Hawthornthwaite-Lawless, A. M.; Papiz, M. Z.; Cogdell, R. J.; Isaacs, N. W. *Nature* **1995**, *374*, 517–521. (b) At 2.0 Å resolution: Papiz, M. Z.; Prince, S. M.; Howard, T.; Cogdell, R. J.; Isaacs, N. W. *J. Mol. Biol.* **2003**, *326*, 1523–1538. (c) The LH2 of the purple bacterium *Rhodospirillum molischianum*: Koepke, J.; Hu, X.; Muenke, C.; Schulten, K.; Michel, H. *Structure* **1996**, *4*, 581–597. (d) LH1-RC: Roszak, A. W.; Howard, T. D.; Southall, J.; Gardiner, A. T.; Law, C. J.; Isaacs, N. W.; Cogdell, R. J. *Science* **2003**, *302*, 1969–1972. (e) PSI: Jordan, P.; Fromme, P.; Witt, H.-T.; Klukas, O.; Saenger, W.; Krauss, N. *Nature* **2001**, *411*, 909–917. (f) PSI-LH1: Ben-Shem, A.; Frolow, F.; Nelson, N. *Nature* **2003**, *426*, 630–635. (g) Plant LHC-II at 2.72 Å resolution: Liu, Z.; Yan, H.; Wang, K.; Kuang, J.; Gui, L.; An, X.; Chang, W. *Nature* **2004**, *428*, 287–292. (h) Plant LHC-II at 2.5 Å resolution: Standfuss, J.; Terwisscha van Scheltinga, A. C.; Lamborghini, M.; Kühlbrandt, W. *EMBO J.* **2005**, *24*, 919–928. (j) PSII at 3.5 Å resolution: Ferreira, K. N.; Iverson, T. M.; Maghlaoui, K.; Barber, J.; Iwata, S. *Science* **2004**, *303*, 1831–1838. (k) PSII at 3.0 Å resolution: Loll, B.; Kern, J.; Saenger, W.; Zouni, A.; Biesiadka, J. *Nature* **2005**, *438*, 1040–1044. (l) PSII at 2.9 Å resolution: Guskov, A.; Kern, J.; Gabdulkhakov, A.; Broser, M.; Zouni, A.; Saenger, W. *Nature Stuct. Mol. Biol.* **2009**, *16*, 334–342.
(5) Bahatyrova, S.; Frese, R. N.; Siebert, C. A.; Olsen, J. D.; van der Werf, K.; van Grondelle, R.; Niederman, R. A.; Bullough, P. A.; Otto, C.; Hunter, C. N. *Nature* **2004**, *430*, 1058–1062.
(6) (a) Manske, A. K.; Glaeser, J.; Kuypers, M. M. M.; Overmann, J. *Appl. Environ. Microbiol.* **2005**, *71*, 8049–8060. (b) Beatty, J. T.; Overmann, J.; Lince, M. T.; Manske, A. K.; Lang, A. S.; Blankenship, R. E.; Van Dover, C. L.; Martison, T. A.; Plumley, F. G. *Proc. Natl. Acad. Sci.U.S.A.* **2005**, *102*, 9306–9310.
(7) (a) Bystrova, M. I.; Mal'gosheva, I. N.; Krasnovskii, A. A. *Mol. Biol.* **1979**, *13*, 440–451. (b) Smith, K. M.; Kehres, L. A. *J. Am. Chem. Soc.* **1983**, *105*, 1387–1389. (c) Brune, D. C.; King, G. H.; Blankenship, R. E. In *Photosynthetic Light-Harvesting Systems*; Scheer, H., Schneider, S., Eds.; Walter de Gruyter: Berlin, 1988; pp 141−151. (d) Holzwarth, A. R.; Griebenow, K.; Schaffner, K. *Z. Naturforsch.* **1990**, *45c*, 203–206. (e) Balaban, T. S.; Holzwarth, A. R.; Schaffner, K.; Boender, G.-J.; de Groot, H. J. M. *Biochemistry* **1995**, *34*, 15259–15266. (f) Balaban, T. S.; Leitich, J.; Holzwarth, A. R.; Schaffner, K. *J. Phys. Chem.* **2000**, *104*, 1362–1372. (g) Pšenčik, J.; Ikonen, T. P.; Laurinmäki, P.; Merckel, M. C.; Butcher, S. J.; Serimaa, R. E.; Tuma, R. *Biophys. J.* **2004**, *87*, 1165–1172. (h) For an excellent review, see: Frigaard, N.-U.; Bryant, D. In *Microbiology Monographs*; Shively, J. M., Ed.; Springer: Berlin, 2006; Vol. 2, pp 79−114. (i) For a very recent novel chlorosome model and discussion of previous models, see: Ganapathy, S.; Oostergetel, G. T.; Wawrzyniak, P. K.; Reus, M.; Maqueo Chew, A. G.; Buda, F.; Boekema, E. J.; Bryant, D. A.; Holzwarth, A. R.; de Groot, H. J. M. *Proc. Natl. Acad. Sci. U.S.A.* **2009**, *106*, 8525–8530.
(8) Olson, J. M. In *The Photosynthetic Bacteria*; Clayton, R. K., Sistrom, W. R., Eds.; Plenum: New York, 1978; pp 161−178.
(9) Fenna, R. E.; Mathews, B. W. *Nature* **1975**, *258*, 573–577. For a more recent structure from a different bacterium, see: Li, Y.-F.; Zhou, W.; Blankenship, R. E.; Allen, J. P. *J. Mol. Biol.* **1997**, *271*, 456–471.
(10) (a) Balaban, T. S.; Bhise, A. D.; Fischer, M.; Linke-Schaetzel, M.; Roussel, C.; Vanthuyne, N. *Angew. Chem., Int. Ed.* **2003**, *42*, 2140–2144. (b) Balaban, T. S.; Bhise, A. D.; Linke-Schaetzel, M.; Vanthuyne, N.; Roussel, C. *Eur. J. Org. Chem.* **2004**, 3919–3930. (c) Balaban, T. S.; Linke-Schaetzel, M.; Bhise, A. D.; Vanthuyne, N.; Roussel, C.; Anson, C. A.; Buth, G.; Eichhöfer, A.; Foster, K.; Garab, G.; Gliemann, H.; Goddard, R.; Javorfi, T.; Powell, A. K.; Rösner, H.; Schimmel, Th. *Chem.−Eur. J.* **2005**, *11*, 2267–2275. (d) Balaban, T. S. *Acc. Chem. Res.* **2005**, *38*, 612–623. (e) Balaban, M. C.; Balaban, T. S. *J. Porph. Phthal.* **2007**, *11*, 277–286. (f) Jochum, T.; Malla Reddy, C.; Eichhöfer, A.; Buth, G.; Szmytkowski, J.; Kalt, H.; Moss, D.; Balaban, T. S. *Proc. Natl. Acad. Sci. U.S.A.* **2008**, *105*, 12736–12741, and references therein.

of proteins[11] or dendrimers.[12] If practical applications are envisaged, efficient synthetic methods, including optimized HPLC separations, and/or stereoselective syntheses have to be developed for accessing enantiopure compounds in sufficient quantities. Stereochemical challenges are that *BChl*s *c*, *d*, and *e* have three chiral centers (asterisks in Chart 1), neglecting the asymmetric carbon atoms of the lipophilic long-chain alcohol residue (e.g., in phytol), and that the central magnesium atom becomes an additional stereogenic element upon axial coordination.[13] In the chlorosomes, both epimers of the 3-(1-hydroxyethyl) group are present in varying amounts, and their exact role in determining the supramolecular architecture is still poorly understood. It has been demonstrated that, by exposing bacterial cultures to different light intensities, the ratio of the 3^1-epimers is drastically affected.[14]

In the present study we have optimized both chiral HPLC conditions and an enantioselective monoreduction which permits preparation of enantiopure self-assembling *BChl d* mimics. In addition, we have assigned the configuration at the sole 3^1-stereocenter by independent chemical and spectroscopic methods, which all lead to the same result. Subsequently, we have investigated the self-assembly properties of the separated enantiomers by stationary absorption, fluorescence, and circular dichroism (CD) spectroscopy and by scanning tunneling electron microscopy (STEM).

Related work by three other groups deserves mention in this context: (i) Tamiaki et al.[15] and, more recently, (ii) Würthner et al.[16] have used mainly semisynthetic approaches starting with algal *Chl a* to obtain self-assembling chlorins; (iii) Lindsey and co-workers[17] have established novel synthetic methods that could easily be adapted to obtain self-assembling porphyrins and chlorins with geminal dimethyl groups which prevent the sometimes spontaneous aerial oxidation of chlorins to porphyrins, thus providing pure and stable compounds with a red-shifted and increased absorption in the vis−NIR region in comparison to that of porphyrins.

Results and Discussion

To equip porphyrins with recognition groups capable of assembling supramolecular architectures, we started with the preformed porphyrin, which was then functionalized.[18] This strategy allowed for the usual lower-yielding porphyrin-forming reactions to occur at the beginning of synthetic sequences, which thus permits improved atom management. Scheme 1 presents the main synthetic transformations for obtaining the self-assembling *BChl* mimics addressed in this work.

Diacetylations of 1-Cu. Porphyrin **1** as a free base (**1-H_2**, M = H_2) can be easily obtained at a gram scale by the condensation of dipyrromethane with 3,5-di-*tert*-butylbenzaldehyde with Lewis ($BF_3 \cdot OEt_2$) or Brønsted (TFA) acid catalysis using the moderately high dilution method (10^{-2} M) in dichloromethane, at room temperature, optimized by Lindsey and co-workers.[19] By this method, reproducible yields of 35−40% are attainable. We usually employ an oven-dried 10-L flask and use technical dichloromethane previously dried over calcium chloride and deoxygenated by passing a stream of argon through a sintered

(11) For polypeptide maquettes or myoglobin-binding tetrapyrrolic chromophores, see: (a) Discher, B. M.; Noy, D.; Strzalka, J.; Moser, C. C.; Lear, J. D.; Blasie, J. K.; Dutton, P. L. *Biochemistry* **2005**, *44*, 12329–12343. (b) Noy, D.; Discher, B. M.; Rubtsov, I. V.; Hochstrasser, R. M.; Dutton, P. L. *Biochemistry* **2005**, *44*, 12344–12354. (c) Pröll, S.; Wilhelm, B.; Robert, B.; Scheer, H. *Biochim. Biophys. Acta (Bioenergetics)* **2006**, *1757*, 750–763. (d) Marković, D.; Pröll, S.; Bubenzer, C.; Scheer, H. *Biochim. Biophys. Acta (Bioenergetics)* **2007**, *1767*, 897–904.

(12) (a) Gensch, T.; Hofkens, J.; Herrmann, A.; Tsuda, K.; Verheijen, W.; Vosch, T.; Christ, T.; Basché, T.; Müllen, K.; De Schryver, F. C. *Angew. Chem., Int. Ed.* **1999**, *38*, 3752–3756. (b) Bhyrappa, P.; Vaijayanthimala, G.; Suslick, K. S. *J. Am. Chem. Soc.* **1999**, *121*, 262–263. (c) Adronov, A.; Gilat, S. L.; Fréchet, J. M. J.; Ohta, K.; Neuwahl, F. V. R.; Fleming, G. R. *J. Am. Chem. Soc.* **2000**, *122*, 1175–1185. (d) Adronov, A.; Gilat, S. L.; Fréchet, J. M. J.; Ohta, K.; Neuwahl, F. V. R.; Fleming, G. R. *J. Am. Chem. Soc.* **2000**, *122*, 1175–1185. (e) Weil, T.; Wiesler, U. M.; Herrmann, A.; Baur, R.; Hofkens, J.; De Schryver, F. C.; Müllen, K. *J. Am. Chem. Soc.* **2001**, *123*, 8101–8108. (f) Weil, T.; Reuther, E.; Müllen, K. *Angew. Chem., Int. Ed.* **2002**, *41*, 1900–1904. (g) Lee, L. F.; Adronov, A.; Schaller, R. D.; Fréchet, J. M. J.; Saykally, R. J. *J. Am. Chem. Soc.* **2003**, *125*, 536–540. (h) Ballester, P.; Gomila, R. M.; Hunter, C. A.; King, A. S. H.; Twyman, L. J. *Chem. Commun.* **2003**, 38–39. (i) Schweitzer, G.; Gronheid, R.; Jordens, S.; Lor, M.; De Belder, G.; Weil, T.; Reuther, E.; Müllen, K.; De Schryver, F. C. *J. Phys. Chem. A* **2003**, *107*, 3199–3207. (j) Metivier, R.; Kulzer, F.; Weil, T.; Müllen, K.; Basché, T. *J. Am. Chem. Soc.* **2004**, *126*, 14364–14365. (k) Weil, T.; Reuther, E.; Beer, C.; Müllen, K. *Chem.—Eur. J.* **2004**, *10*, 1398–1414. (l) Herrmann, A.; Müllen, K. *Chem. Lett.* **2006**, *35*, 978–986. (m) Flors, C.; Oesterling, I.; Schnitzler, T.; Fron, E.; Schweitzer, G.; Sliwa, M.; Herrmann, A.; van der Auweraer, M.; de Schryver, F. C.; Müllen, K.; Hofkens, J. *J. Phys. Chem. C* **2007**, *111*, 4861–4870.

(13) (a) Balaban, T. S. *Photosynth. Res.* **2005**, *86*, 251–262. (b) Oba, T.; Tamiaki, H. *Bioorg. Med. Chem.* **2005**, *13*, 5733–5739.

(14) (a) Bobe, F. W.; Pfennig, N.; Swanson, K. L.; Smith, K. M. *Biochemistry* **1990**, *29*, 4340–4348. (b) Borrego, C. M.; Gerola, P. D.; Miller, M.; Cox, R. P. *Photosynth. Res.* **1999**, *59*, 159–166. (c) Steensgaard, D. B.; Wackerbarth, H.; Hildebrandt, P.; Holzwarth, A. R. *J. Phys. Chem. B* **2000**, *104*, 10379–10386. (d) Ishii, T.; Kimura, M.; Yamamoto, T.; Kirihata, M.; Uehara, K. *Photochem. Photobiol.* **2000**, *71*, 567–573.

(15) (a) Balaban, T. S.; Tamiaki, H.; Holzwarth, A. R.; Schaffner, K. *J. Phys. Chem.* **1997**, *101*, 3424–3431. (b) Miyatake, T.; Tamiaki, H.; Holzwarth, A. R.; Schaffner, K. *Helv. Chim. Acta* **1999**, *82*, 797–810. (c) Miyatake, T.; Oba, T.; Tamiaki, H. *ChemBioChem* **2001**, 335–342. (d) Yagai, S.; Tamiaki, H. *J. Chem. Soc., Perkin Trans.1* **2001**, 3135–3144. (e) Yagai, S.; Miyatake, T.; Tamiaki, H. *J. Org. Chem.* **2002**, *67*, 49–58. (f) de Boer, I.; Matysik, J.; Amakawa, M.; Yagai, S.; Tamiaki, H.; Holzwarth, A. R.; de Groot, H. J. M. *J. Am. Chem. Soc.* **2003**, *125*, 13374–13375. (g) Kunieda, M.; Mizoguchi, T.; Tamiaki, H. *Photochem. Photobiol.* **2004**, *7*, 55–61. (h) Sasaki, S.; Tamiaki, H. *Bull. Chem. Soc. Jpn.* **2004**, *77*, 797–800. (i) Kunieda, M.; Tamiaki, H. *J. Org. Chem.* **2005**, *70*, 820–828. (j) Miyatake, T.; Tamiaki, H. *J. Photochem. Photobiol. C: Photochem. Rev.* **2005**, *6*, 89–107. (k) Sasaki, S.; Tamiaki, H. *J. Org. Chem.* **2006**, *71*, 2648–2654. (l) Mizoguchi, T.; Shoji, A.; Kunieda, M.; Miyashita, H.; Tsuchiya, T.; Mimuro, M.; Tamiaki, H. *Photochem. Photobiol. Sci.* **2006**, *5*, 291–299. (m) Saga, Y.; Kim, T.-Y.; Hisai, T.; Tamiaki, H. *Thin Solid Films* **2006**, *500*, 278–282. (n) Tamiaki, H.; Michitsuji, T.; Shibata, R. *Photochem. Photobiol. Sci.* **2008**, *7*, 1225–1230. (o) Kunieda, M.; Tamiaki, H. *J. Org. Chem.* **2008**, *73*, 7686–7694. (p) Mizoguchi, T.; Kim, T.-Y.; Sawamura, S.; Tamiaki, H. *J. Phys. Chem. B* **2008**, *112*, 16759–16765.

(16) (a) Röger, C.; Müller, M.; Lysetska, M.; Miloslavina, Y.; Holzwarth, A. R.; Würthner, F. *J. Am. Chem. Soc.* **2006**, *128*, 6542–6543. (b) Röger, C.; Miloslavina, Y.; Brunner, D.; Holzwarth, A. R.; Würthner, F. *J. Am. Chem. Soc.* **2008**, *130*, 5929–5939. (c) Huber, V.; Sengupta, S.; Würthner, F. *Chem.—Eur. J.* **2008**, *14*, 7791–7807. (d) Ganapathy, S.; Sengupta, S.; Wawrzyniak, P. K.; Huber, V.; Buda, F.; Baumeister, U.; Würthner, F.; de Groot, H. J. M. *Proc. Natl. Acad. Sci. U.S.A.* **2009**, *106*, 11472–11477.

(17) (a) Yao, Z.; Bhaumik, J.; Dhanalekshmi, S.; Ptaszek, M.; Rodriguez, P. A.; Lindsey, J. S. *Tetrahedron* **2007**, *63*, 10657–10670. (b) Ptaszek, M.; Yao, Z.; Savithri, D.; Boyle, P. D.; Lindsey, J. S. *Tetrahedron* **2007**, *63*, 12629–12638. (c) Lindsey, J. S.; Chinnasamy, M.; Fan, D. U.S. Patent US2008/0029155 A1, February 7, 2008.

(18) (a) Balaban, T. S.; Goddard, R.; Linke-Schaetzel, M.; Lehn, J.-M. *J. Am. Chem. Soc.* **2003**, *125*, 4233–4239. (b) Balaban, T. S.; Eichhöfer, A.; Krische, M. J.; Lehn, J.-M. *Helv. Chim. Acta* **2006**, *89*, 333–351.

(19) (a) Lindsey, J. S.; Schreiman, I. C.; Hsu, H. C.; Kearney, P. C.; Marguerettaz, A. M. *J. Org. Chem.* **1987**, *52*, 827–836. (b) Littler, B. J.; Miller, M. A.; Hung, C.-H.; Wagner, R. W.; O'Shea, D. F.; Boyle, P. D.; Lindsey, J. S. *J. Org. Chem.* **1999**, *64*, 1391–1396. (c) Littler, B. J.; Ciringh, Y.; Lindsey, J. S. *J. Org. Chem.* **1999**, *64*, 2864–2872.

Scheme 1[a]

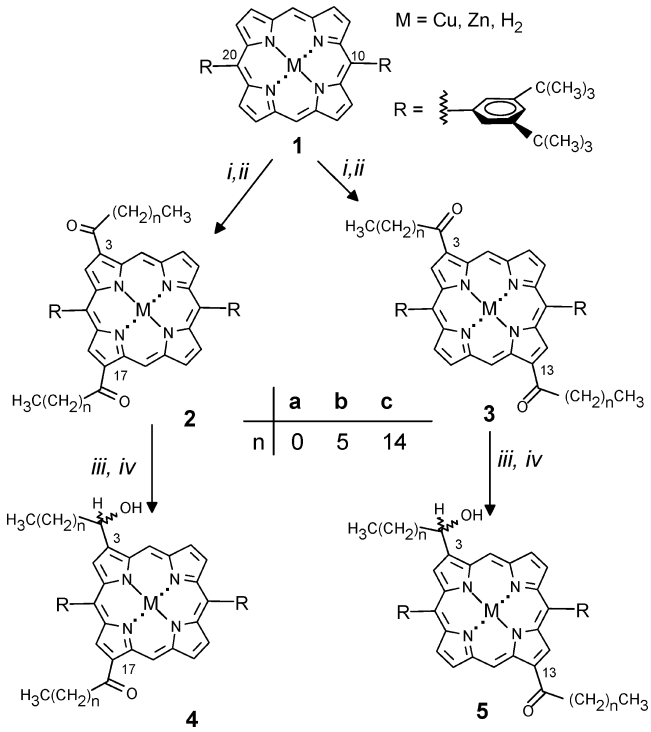

[a] Reagents and conditions for each step are as follow. (*i*) Diacylation: $H_3C-COCl$, $AlCl_3$, CS_2, 0−5 °C or Ac_2O, $SnCl_4$, CS_2. (*ii*) Copper demetalation: TFA:H_2SO_4, 1:1 v/v, room temperature. (*iii*) Statistical monoreduction: $NaBH_4$, MeOH, CH_2Cl_2 or $CHCl_3$, room temperature. (*iv*) Zinc metalation: $Zn(OAc)_2$, $CHCl_3$:MeOH, 4:1 v/v.

glass frit immersed directly in the reaction vessel, which is protected from light by an aluminum foil. Oxidation of the intermediate porphyrinogen is more convenient with 2,3-dichloro-5,6-dicyano-*p*-benzoquinonone (DDQ) than with *p*-chloranil due to the easier chromatographic separation of the product **1-H$_2$**. For Friedel−Crafts diacetylation or Vilsmeier diformylation, the free-base porphyrin needs to be metalated with copper acetate under standard conditions.[20] Interestingly, while **1-Cu** is 5-monoformylated and 5,15-diformylated—i.e., the Vilsmeier reagent attacks the more reactive free *meso* positions—Friedel−Crafts acylations occur preferentially at the β-pyrrolic positions (*vide infra*).

The 3,5-di-*tert*-butylphenyl group, which was introduced into porphyrin chemistry by Crossley,[21] has several advantages: (i) due to steric hindrance by the *tert*-butyl groups, the phenyl substituents are inert in electrophilic substitution reactions, which can thus attack exclusively the porphyrin macrocycle; (ii) the 2, 8, 12, and 18 positions of the porphyrin are also within the sterical shielding cone of the frequently rotating (on the NMR time scale) 10,20-di-*tert*-butylphenyl groups, so that these β-pyrrolic positions are not attacked by acylium ions in Friedel−Crafts acylations; (iii) it induces high solubility in medium-polarity and nonpolar solvents and inhibits aggregation by π-stacking of the macrocyles; (iv) it packs well in crystal lattices, thus permitting good-quality single crystals to be obtained which are amenable to X-ray analyses; and (v) due to the intense ^{1}H NMR singlet(s), it allows easy detection at submicromolar concentrations of products in complex reaction mixtures and sometimes it gives a hint at the symmetry of the product due to the aniso- or isochronous character of the *tert*-butyl groups (*vide infra*).

Diacetylation of **1-Cu** with an excess of acetic anhydride and tin tetrachloride as the Friedel−Crafts catalyst at 0−3 °C for 30 min gave an almost equimolar mixture (44:56) of the 3,17- and 3,13-diacetyl-substituted porphyrins **2a-Cu** and **3a-Cu**. The yields over different runs were consistently over 27%, with ∼35% yields when carbon disulfide was used as the solvent. Under these conditions, both diacetylated isomers were obtained, and their separation was achieved by careful column chromatography on silica gel after demetalation. By stirring at room temperature for 90 min with a degassed mixture of concentrated sulfuric and trifluoroacetic acids, high demetalation yields (e.g., 98%) of the corresponding free bases, **2a-H$_2$** and **3a-H$_2$**, were achieved at a 600-mg scale. Yields tended to decrease when working at larger scales, e.g., 86% for a 1.5-g mixture of **2a-Cu** and **3a-Cu**. The chromatographic separation worked better for the free bases than for their copper or zinc complexes, and by elution with dichloromethane from silica gel, the reddish 3,17-diacetyl isomer **2a-H$_2$** was eluted first, followed closely by the greenish 3,13-diacetyl isomer **3a-H$_2$**. On a preparative HPLC SiO_2 Dynamax 100-Å column run with 3% 2-propanol in dichloromethane, the elution order was reversed for the copper complexes, i.e., **3a-Cu** eluted before **2a-Cu**. On the same column, baseline separation was achieved with an isocratic elution using dichloromethane/*n*-hexane (1:1 v/v) for the corresponding free bases, with **2a-H$_2$** eluting before **3a-H$_2$**.

Acetylations of geoporphyrins have been described by Callot and co-workers.[22] By adapting their procedure, with only a slight excess of acetic anhydride and short reaction times (2−10 min), monoacetylation of **1-Cu** occurred, which permitted isolation of the 3-acetyl copper porphyrin in fair yields. This compound could be subjected to a second and different acylation step; its Vilsmeier formylation failed, however, to give the 3-acetyl-15-formyl copper porphyrin. The latter compound was conveniently prepared by reversing the order and performing first the mono-*meso*-formylation of **1-Cu**, followed by the Friedel−Crafts monoacetylation.[23]

Diacylations of **1-Cu** were undertaken by using several acyl chlorides and $AlCl_3$ in carbon disulfide at 0−5 °C. After short reaction times and in concentrated CS_2 solutions (∼5 mM), in less than 5 min, the 3,17-diacyl isomers **2a-c-Cu** were formed preferentially and could be isolated virtually free of the 3,13-isomers. At higher temperatures and longer reaction times, the 3,13-diacyl isomers **3a-c-Cu** were formed as the minor products. In more dilute solutions (<0.1 mM), the reaction is slower and can be stopped before the 3,13-diacyl isomer starts to be formed. Other acyl chlorides, e.g., butyroyl to myristoyl chloride, behaved similarly.[23] It was thus quite remarkable that, out of the 12 possible diacylated isomers of **1-Cu**, one can drive the reaction regiospecifically to obtain the 3,17-diacyl isomer as

(20) (a) Smith, K. M.; Bisset, G. M. F.; Case, J. J.; Tabba, H. D. *Tetrahedron Lett.* **1980**, *21*, 3747–3750. (b) Smith, K. M.; Bisset, G. M. F.; Tabba, H. D. *J. Chem. Soc., Perkin Trans. 1* **1982**, *1982*, 581–585.

(21) (a) Crossley, M. J.; Burn, P. L. *J. Chem. Soc., Chem. Commun.* **1987**, 39–40. (b) Crossley, M. J.; Burn, P. L. *J. Chem. Soc., Chem. Commun.* **1991**, 1569–1571. (c) Reimers, J. R.; Lü, T. X.; Crossley, M. J.; Hush, N. S. *Nanotechnology* **1996**, *7*, 424–429.

(22) (a) Jeandon, C.; Bauder, C.; Callot, H. J. *Energy Fuels* **1990**, *4*, 665–667. (b) Jeandon, C.; Ruppert, R.; Callot, H. J. *J. Org. Chem.* **2006**, *71*, 3111–3120.

(23) Bhise, A. D. Ph.D. Thesis, Universität Karlsruhe (TH), 2005 (Wissenschaftliche Berichte FZKA 7174, ISSN 0947-8620).

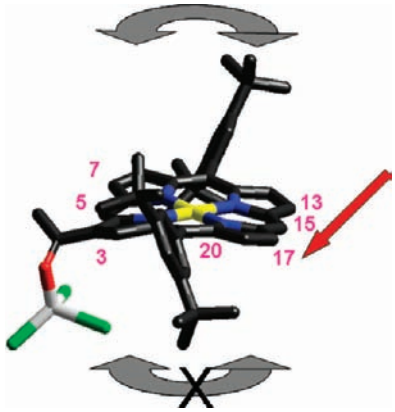

Figure 1. Mechanistic explanation of preferential formation of the 3,17-diacylporphyrins. Color coding: carbon, black; oxygen, red; nitrogen, blue; copper, yellow; aluminum, light gray; and chlorine, green. Hydrogen atoms have been omitted for clarity.

the only product. A plausible mechanistic explanation for this astonishing regioselectivity follows and is illustrated in Figure 1.

The acylium cation attacks the most reactive position on the porphyrin periphery, which has to be one of the two free *meso*-positions. The 5-*meso*-π-complex can decay to the σ-complex, which, however, due to steric hindrance with the two adjacent β-pyrrolic protons, cannot lead to an acyl group in conjugation with the porphyrin macrocycle. Indeed, our *meso*-acetyl compounds, obtained by an indirect method,[10a] have been proven by X-ray crystallography to have perpendicular carbonyl groups and are red colored.[10c] *meso*-Formyl porphyrins, on the other hand, are green colored, and the formyl group is in the porphyrin plane, fully conjugated,[10b] which is also supported by FT-IR data.[10f] Thus, the 5-*meso*-π-complex prefers to shift to a 3-acyl-π-complex, where substitution can now occur with formation of the conjugated carbonyl group, and this product can also be isolated. Why does the diacylation favor the formation of the 3,17-diacyl compounds when the 3,13- or even 3,7-diacylated product should be equally stable according to semiempirical PM3 calculations?[24] We exclude that the square planar copper ion plays a role in chelating the acylium chloroaluminate acylating agent. Rather, as usual with stoichiometric $AlCl_3$ acylations, the 3-acyl group will strongly complex $AlCl_3$. This leads to severe steric hindrance of both a renewed attack in the *meso*-5 position and the rotation of the neighboring 20-di-*tert*-butylphenyl group, which must reside in a frozen twisted conformation (see Supporting Information, Figure S17, for conformational analyses). The second acylium ion will thus preferentially enter the only other available *meso*-position (15). The shift of this latter π-complex can occur more rapidly to the adjacent 17-β-pyrrolic position, indicated by the red arrow in Figure 1, which is opened up by the blocked 20-di-*tert*-butylphenyl group. Migration to the 13-position occurs more slowly due to the more frequently rotating 10-di-*tert*-butylphenyl group.

The structural assignment can be deduced quite straightforwardly from the ^{1}H NMR spectra of the free bases, since compounds **2a-c-H$_2$** have nonequivalent 10- and 20-(3,5-di-*tert*-butylphenyl) groups. The splitting of the phenyl protons is exemplarily shown in Figure 2 for **2a-H$_2$** in comparison with **3a-H$_2$**.

(24) *HyperChem Program Package*, version 7.5; HyperCube Inc.: Gainesville, FL, 2003.

The 3,17-diacetyl free-base **2a-H$_2$** gave crystals suitable for X-ray structure analysis, which unequivocally proved the structure as shown in Figure 3. The two acetyl groups are oriented in opposite directions, both being coplanar with the porphyrin macrocycle. This arrangement minimizes the dipole moment within the monomeric unit. Interestingly, extensive π-stacking occurs with a 3.55-Å interplanar distance within strongly coupled dimers having the acetyl groups in non-overlapping positions. Within such dimers, the total dipole moment is entirely averaged out. This large degree of π-overlap, which is uncommon because usually porphyrins tend to stack with an offset geometry,[25] is due to the electron-withdrawing effect of the two acetyl groups, which makes the porphyrin rings π-poor, minimizing their repulsion and allowing them to come close to each other.

Monoreductions of Diacetyl Porphyrins 2a-H$_2$ and 3a-H$_2$. With the pure diacetyl porphyrins in hand, we performed the reduction of one acyl group to a hydroxyalkyl substituent. The two acetyl groups being equivalent (homotopic), the statistical monoreduction of any of them leads to the same product. These reactions were easily monitored by TLC, as the retention factors of the monoalcohol (ketol) and especially of the diol species were much smaller than those of the starting diacyl compounds. The reduction with $NaBH_4$ in a dichloromethane or chloroform/methanol mixture (4:1 v/v) could be stopped after the appearance of the two spots corresponding to the racemic (*RR*/*SS*) and *meso*-diol (*RS*) compounds at about 65−80% conversion of the diacetylated porphyrins. It was very fortunate that the monoalcohol could be isolated. This was probably due to the mutual activation of the two acetyl groups toward nucleophilic reduction. Once the first acetyl group was reduced, the second one reacted more sluggishly.

Among different possible reagents and conditions for the enantioselective monoreduction of the diacetylated porphyrins **2a-H$_2$** and **3a-H$_2$**,[26] the Corey−Bakshi−Shibata reagent {CBS, (3a*S*)- or (3a*R*)-1-methyl-3,3-diphenyltetrahydro-3*H*-pyrrolo[1,2-*c*][1,3,2]oxazaborrole}, which had previously been employed by Montforts in the synthesis of hematoporphyrin stereoisomers,[27] gave the best results. Under our optimized conditions, which consisted of reacting **2a-H$_2$** in toluene at −80 °C for 1 h with 1 equiv of (*R*)-CBS and 4 equiv of catecholborane, we attained a 42% yield and 79% ee of the (*S*)-3-(1-hydroxyethyl)porphyrin **4a-H$_2$** (for assignments of the configuration at the 3^1-stereocenter, see the next section). The (*S*)-CBS reductions consistently gave lower ee's; we explain this by the variable quality of the respective commercial reagents, which in this case are not derived from the natural chiral pool. To our disappointment, under the same conditions, reaction of **3a-H$_2$** with 1 equiv of (*R*)-CBS, when compared to **4a-H$_2$**, proceeded more slowly and in lower yield (32%) and only to 54% ee. With 1 equiv of (*S*)-CBS, the yield was only 22% and the ee was 36%. Higher reaction temperatures or other commercial amine−borane or dimethylsulfide−borane complexes, although sometimes giving higher yields, led to the sacrifice of the ee values.

Due to progress in separation techniques, including their upscaling, in order to obtain enantiopure *BChl* mimics, it appears

(25) Hunter, C.; Sanders, J. K. M. *J. Am. Chem. Soc.* **1990**, *112*, 5525–5534.
(26) Mössinger, D. Diploma Thesis, Universität Karlsruhe (TH), 2006.
(27) (a) Kusch, D.; Töllner, E.; Lincke, A.; Montforts, F.-P. *Angew. Chem., Int. Ed. Engl.* **1995**, *34*, 784–787. (b) Kusch, D.; Montforts, F.-P. *Tetrahedron: Asymmetry* **1995**, *6*, 867–870. (c) Tamiaki, H.; Kouraba, M.; Takeda, K.; Kondo, S.; Tanikaga, R. *Tetrahedron: Asymmetry* **1998**, *9*, 2101–2111.

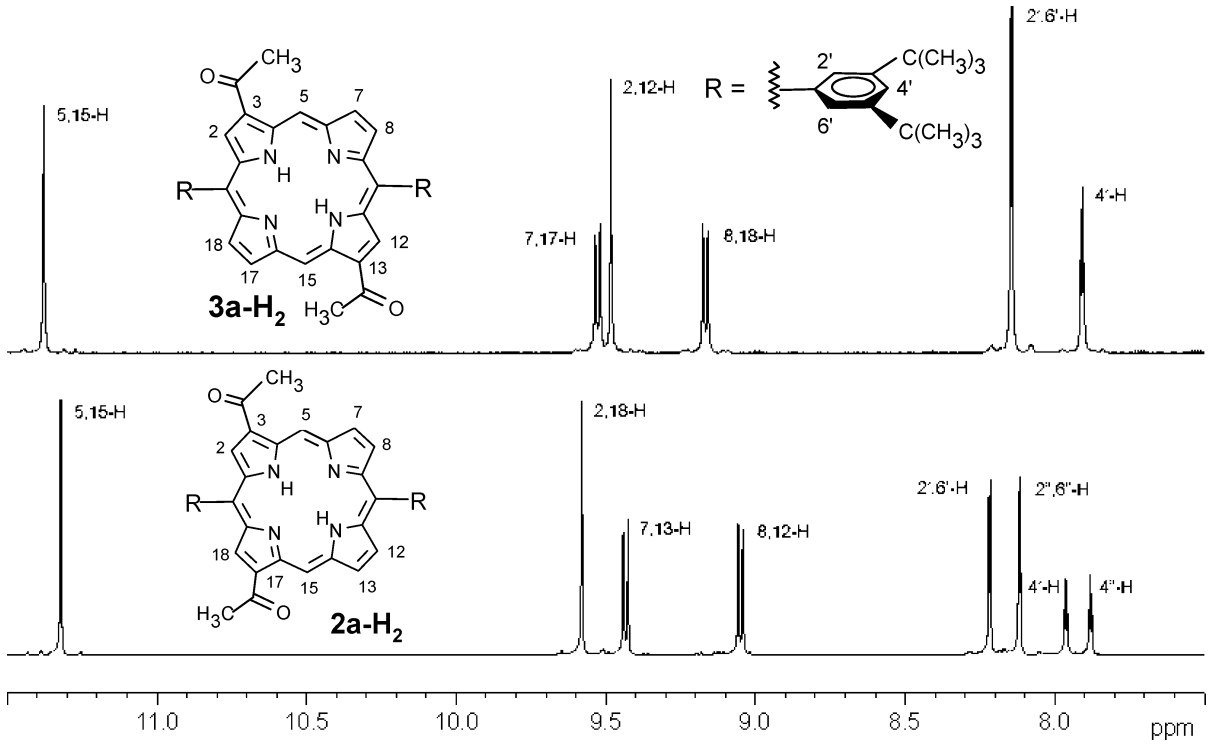

Figure 2. Aromatic region of the 300-MHz ^{1}H NMR spectra in $CDCl_3$ of **2a-H$_2$** (bottom trace) in comparison with **3a-H$_2$** (top). For the full spectra, including other examples, see the Supporting Information, Figures S5−S7.

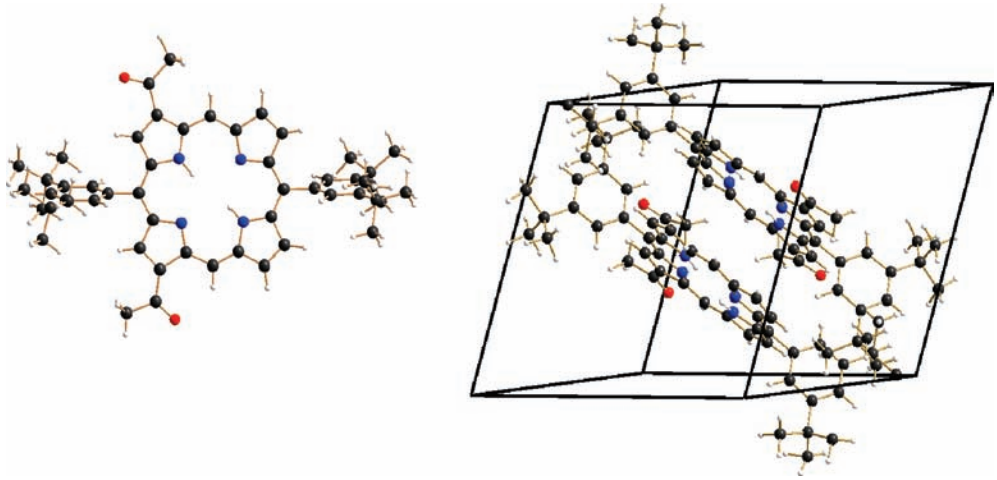

Figure 3. (Left) Monomeric unit of **2a-H$_2$** and (right) the unit cell, which comprises a π-stacked dimer. Details of the data collection and crystallographic analysis are given in the Supporting Information.

advantageous to use the cheap reducing reagent $NaBH_4$, giving rise to the racemate, which then can be quantitatively resolved on a variety of chiral HPLC columns into the pure 3^1-enantiomers in quantitative yields, without any loss of material.

Assignment of the Absolute Configuration at the 3^1-Stereocenter. Chiral HPLC successfully resolved the enantiomers of **4a-H$_2$** and **5a-H$_2$**. Analytical HPLC on 11 chiral stationary phases and a typical chromatogram for **4a-H$_2$** are described in the Supporting Information. In particular, the ULMO (*S*,*S*) column, eluted with ethanol, permitted separation of the enantiomers of **4a-H$_2$** and **5a-H$_2$**. Uray et al.,[28] the inventors of the ULMO (*S*,*S*) stationary phase, reported the order of elution for more than 15 benzylic secondary alcohols on this column. On the basis of the finding that the (*R*)-enantiomers always eluted first, we can assume that the "faster" enantiomers of **4a-H$_2$** and **5a-H$_2$** on ULMO (*S*,*S*) also have a (3^1*R*) absolute configuration. However, assignment of the absolute configuration from the elution order obtained by chiral HPLC must be done cautiously[29] and needs to be validated by other methods.

Our above preliminary assignment was actually confirmed by the fact that the first eluted enantiomers were identical to those formed stereoselectively by the monoreduction of the

(28) (a) Maier, N. M.; Uray, G. *J. Chromatogr. A* **1996**, *732*, 215–230. (b) Uray, G.; Maier, N. M.; Niederreiter, K. S.; Spitaler, M. M. *J. Chromatogr. A* **1998**, *799*, 67–81. (c) Uray, G.; Stampfer, W.; Fabian, W. M. F. *J. Chromatogr. A* **2003**, *992*, 151–157.

(29) Roussel, C.; Del Rio, A.; Pierrot-Sanders, J.; Piras, P.; Vanthuyne, N. *J. Chromatogr. A* **2004**, *1037*, 311–328.

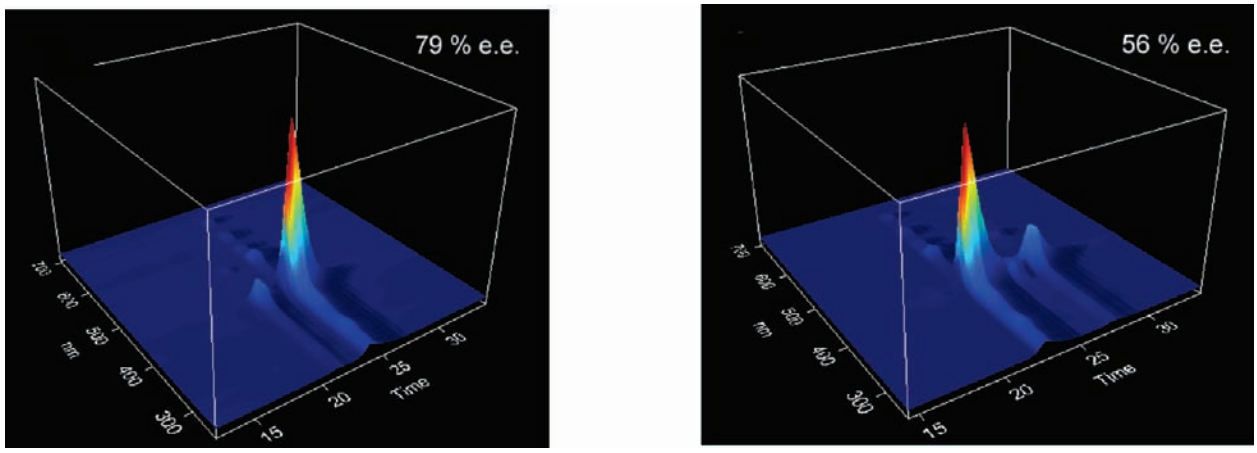

Figure 4. HPLC elution from a chiral ULMO (*S*,*S*) column with *n*-hexane/2-propanol (4:1 v/v), 4 mL/min, and UV−vis absorption spectra of the reduction products of **4a-H$_2$** with 1 equiv of (*R*)-CBS (left) and (*S*)-CBS (right). The sharp Soret band, with higher loadings of the column, sometimes saturates the diode array detector.

corresponding diacetyl compounds employing the (*S*)-CBS reagent (Figure 4). The second eluted enantiomers were those formed predominantly with the (*R*)-CBS reagent and, due to the accepted mechanism of ketone reductions,[30] were thus attributed to the (3^1*S*)-configuration.

For a robust assignment of the absolute stereostructures of the porphyrins synthesized, measurement of circular dichroism (CD) spectra and their interpretation by quantum chemical CD calculations[31] seemed to be the method of choice. However, no significant CD spectra were obtained by standard offline CD measurements of the enantiomers (*R*)-**4a-Zn** (99% ee) and (*S*)-**4a-Zn** (98% ee), which were synthesized by zinc(II) insertion into the previously resolved free bases (*R*)-**4a-H$_2$** and (*S*)-**4a-H$_2$** (see above). In none of the solvents used—dichloromethane, methanol, or 2-propanol—were any clear, reproducible, and thus interpretable CD effects observed. To exclude any interference by possible impurities, we also performed online CD measurements (in the stopped-flow mode), i.e., by HPLC−CD coupling,[31c] but—as for the offline measurements—no CD spectra were obtained.[32] Obviously, the influence of the peripheral, freely rotating stereogenic center on the flat, strongly absorbing chromophore is too small to result in a measurable CD curve for the monomeric, nonaggregated species.[31] Fully in line with this result is the fact that, to the best of our knowledge, no CD spectra of any monomeric porphyrins bearing just one chiral center in an aliphatic side chain have so far been reported in the literature,[33] in contrast to numerous significant CD effects described for various chiral porphyrin derivatives possessing other elements of chirality or having more than one porphyrin residue.[34] Thus, unlike for the self-assembly experiments (see below), the CD effects could not be accurately measured and interpreted.

In order to investigate the configuration at the stereogenic center more closely, two other independent methods were applied, one based on an oxidative degradation of benzylic acetates and ensuing stereoanalysis of the resulting lactic acetates, and the other based on the NMR analysis of the respective Mosher esters.

Assignment of the 3^1-Configuration by Oxidative Degradation. For this purpose, a ruthenium-mediated oxidative degradation procedure developed in Würzburg for chiral benzylic alcohols[35] and related chiral molecules[36,37] was applied to each of the two 3^1-acetoxy-substituted enantiomers of **4a-H$_2$**, resulting in the respective enantiomers of 2-acetoxypropionic acid (**6**, Figure 5), which were both analyzed by GC on a CDX-B chiral phase. The absolute configurations of these enantiomeric 2-acetoxypropionic acids were attributed to the particular signals by GC comparison with racemic 2-acetoxypropionic acid as a reference, with the more rapidly eluting enantiomer being (*R*)-configured and the "slower" one having the (*S*)-configuration.

In the case of the 2-acetoxypropionic acid obtained from the faster eluting enantiomer of **4a-H$_2$**, a single peak was obtained

(30) (a) Corey, E. J.; Helal, C. J. *Angew. Chem., Int. Ed.* **1998**, *37*, 1986–2012. (b) Corey, E. J.; Bakshi, R. K. *Tetrahedron Lett.* **1990**, *31*, 611–614.

(31) (a) Bringmann, G.; Busemann, S. In *Natural Product Analysis*; Schreier, P., Herderich, M., Humpf, H. U., Schwab, W., Eds.; Vieweg: Wiesbaden, 1998; pp 195−212. (b) Bringmann, G.; Gulder, T. A. M.; Reichert, M.; Gulder, T. *Chirality* **2008**, *20*, 628–642. (c) Bringmann, G.; Bruhn, T.; Maksimenka, K.; Hemberger, Y. *Eur. J. Org. Chem.* **2009**, 2717–2727.

(32) (a) The results of the quantum chemical CD calculations performed in parallel thus could not be compared with experimental CD curves and will be reported elsewhere. (b) In a similar way, strongly colored compounds often do not give reliable $[\alpha]_D$ values, due to their intense UV absorption. (c) Mutanyatta, J.; Bezabih, M.; Abegaz, B.; Dreyer, M.; Brun, R.; Kocher, N.; Bringmann, G. *Tetrahedron* **2005**, *61*, 8475–8484. (d) Thomson, R. H. *Naturally Occurring Quinones IV Recent Advances*; Blackie Academic and Professional: London, 1997; p 134. (e) Sharma, P. K.; Khanna, R. N.; Rohatgi, B. K.; Thomson, R. H. *Phytochemistry* **1988**, *27*, 632–633. (f) Khanna, R. N.; Sharma, P. K.; Thomson, R. H. *J. Chem. Soc., Perkin Trans. 1* **1987**, 1821–1824. (g) Capon, R. J.; Groves, D. R.; Urban, S.; Watson, R. G. *Aust. J. Chem.* **1993**, *46*, 1245–1253. (h) Bringmann, G.; Rüdenauer, S.; Götz, D. C. G.; Gulder, T. A. M.; Reichert, M. *Org. Lett.* **2006**, *8*, 4743–4746.

(33) For a review on porphyrins as CD reporter groups, see: Huang, X.; Nakanishi, K.; Berova, N. *Chirality* **2000**, *12*, 237–255.

(34) For some selected, recent examples, see: (a) Borovkov, V. V.; Inoue, Y. In *Supramolecular Chirality*; Crego-Calama, M., Reinhoudt, D. N., Eds.; Topics in Current Chemistry *265*; Springer: Berlin, 2006; pp 89−146. (b) Mizumura, M.; Shinokubo, H.; Osuka, A. *Angew. Chem., Int. Ed.* **2008**, *47*, 5378–5381. (c) Kai, H.; Nara, S.; Kinbara, K.; Aida, T. *J. Am. Chem. Soc.* **2008**, *130*, 6725–6727. (d) Shoji, Y.; Tashiro, K.; Aida, T. *Chirality* **2008**, *20*, 420–424. (e) Bringmann, G.; Götz, D. C. G.; Gulder, T. A. M.; Gehrke, T. H.; Bruhn, T.; Kupfer, T.; Radacki, K.; Braunschweig, H.; Heckmann, A.; Lambert, C. *J. Am. Chem. Soc.* **2008**, *130*, 17812–17825.

(35) Bringmann, G.; Münchbach, M.; Michel, M. *Tetrahedron: Asymmetry* **2000**, *11*, 3167–3176.

(36) Bringmann, G.; God, R.; Schäffer, M. *Phytochemistry* **1996**, *43*, 1393–1403.

(37) Bringmann, G.; Münchbach, M.; Messer, K.; Koppler, D.; Michel, M.; Schupp, O.; Wenzel, M.; Louis, A. M. *Phytochemistry* **1999**, *51*, 693–699.

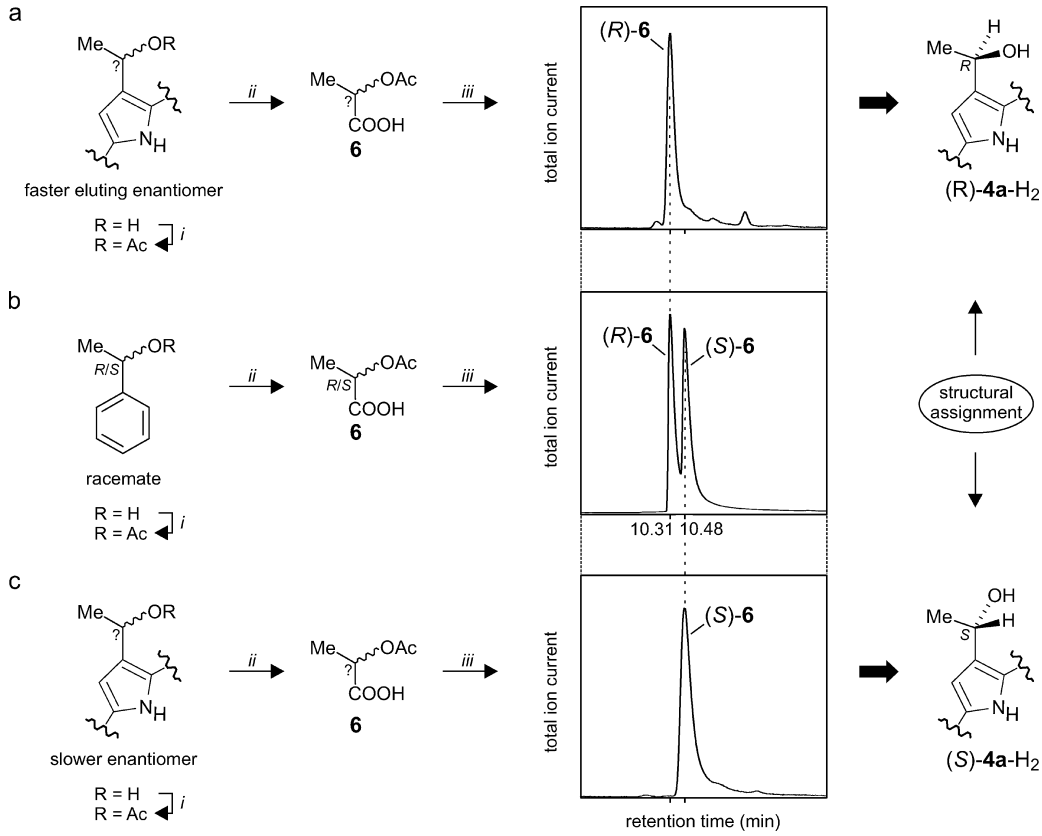

Figure 5. Enantiomeric assignment of the degradation product **6** of the faster enantiomer of **4a-H$_2$** (a) and of the more slowly eluting one (c), by GC analysis in comparison with the standard (b). (*i*) AcCl, NEt_3; (*ii*) $RuCl_3$, $NaIO_4$; (*iii*) GC analysis on a chiral CDX-B phase.

(Figure 5a), having the same retention time as that found for the more rapid (*R*)-enantiomer of 2-acetoxypropionic acid (Figure 5b). This was further confirmed by coelution experiments (see Figure S4, Supporting Information), leading to the assignment of the (*R*)-configuration for this enantiomer. In the other case, a peak coeluting with that originating from (*S*)-2-acetoxypropionic acid was seen (Figure 5c), resulting in the determination that the stereogenic center of the more slowly eluting enantiomer from the ULMO (*S*,*S*) and Whelk (*S*,*S*) stationary phases of **4a-H$_2$** was (*S*)-configured. Therefore, the degradation experiments unambiguously verified the results obtained by the CBS reduction.

Assignment of the 3^1-Configuration Using Mosher's Esters. Recently, a modified Mosher's method was reported to be effective for the configurational assignment of epimerically pure secondary alcohols, including chlorophyll derivatives.[38] Using this method, we investigated three samples resulting from two independent preparative HPLC separations of **4a-H$_2$**. The two HPLC runs were labeled 1 and 2, and the first eluted enantiomer was labeled A, while the second eluted enantiomer was labeled B. Enantiomerically pure A2 was treated with commercially available (+)-MTPA-Cl in dry pyridine to afford the corresponding Mosher's ester, (*R*)-MTPA ester (see Scheme 2). Similarly, reaction of A2 with (−)-MTPA-Cl gave the corresponding (*S*)-MTPA ester. Table S1 in the Supporting Information lists the ^{1}H chemical shifts (δ values) of the (*R*)-MTPA and (*S*)-MTPA esters together with their differences, $\Delta = \delta$[(*S*)-MTPA ester] − δ[(*R*)-MTPA ester]. The δ values for the 3^1-methyl group in (*R*)- and (*S*)-MTPA esters were measured in $CDCl_3$ to be 2.330 and 2.424 ppm, respectively. The value of $\Delta = 2.424 - 2.330 = +0.094$ ppm was positive. By contrast, all the Δ values for the assigned protons on the peripheral positions of the porphyrin π-system gave consistently negative values, which tended to decrease in absolute value with increasing distance from the 3^1-chiral position (Chart 2). According to the modified Mosher rule,[38b] the secondary alcohol was predicted to have the (*R*)-configuration at the 3^1-position. Moreover, the Δ value in the methoxy group of the MTPA esters was positive, +0.174 ppm, indicating that the enantiomerically pure A2 has the (*R*)-configuration at the 3^1-position on the basis of the other modified Mosher rule.[38c]

The other enantiomer from the same run, B2, was esterified with (+)- or (−)-MTPA-Cl to give the corresponding esters (*R*)-MTPA and (*S*)-MTPA, respectively. The modified Mosher method using $\Delta\delta_H$ showed that this enantiomer unambiguously had the *S*-configuration at the 3^1-position (see Chart 2 and Table S1).

As a double-check, another esterified sample from run 1 (B1) was compared with B2; it gave identical results (Table S2, Supporting Information) within 0.004 ppm, allowing us to have a high degree of confidence in the NMR-derived assignments.

Self-Assembly Experiments. With the separated enantiomers of **4a-H$_2$** and **5a-H$_2$** after zinc insertion, which afforded **4a-Zn** and **5a-Zn,** we performed self-assembly experiments in nonpolar solvents. The self-assembled species are characterized by red-shifted maxima, in comparison to the monomers, as in J-

(38) (a) Tamiaki, H.; Kitamoto, H.; Nishikawa, A.; Hibino, T.; Shibata, R. *Bioorg. Med. Chem.* **2004**, *12*, 1657–1666. (b) Ohtani, I.; Kusumi, T.; Kashman, Y.; Kakisawa, H. *J. Am. Chem. Soc.* **1991**, *113*, 4092–4096. (c) Kelly, D. R. *Tetrahedron: Asymmetry.* **1999**, *10*, 2927–2934.

Scheme 2. Synthesis of (*R*)- and (*S*)-Mosher's Esters[a]

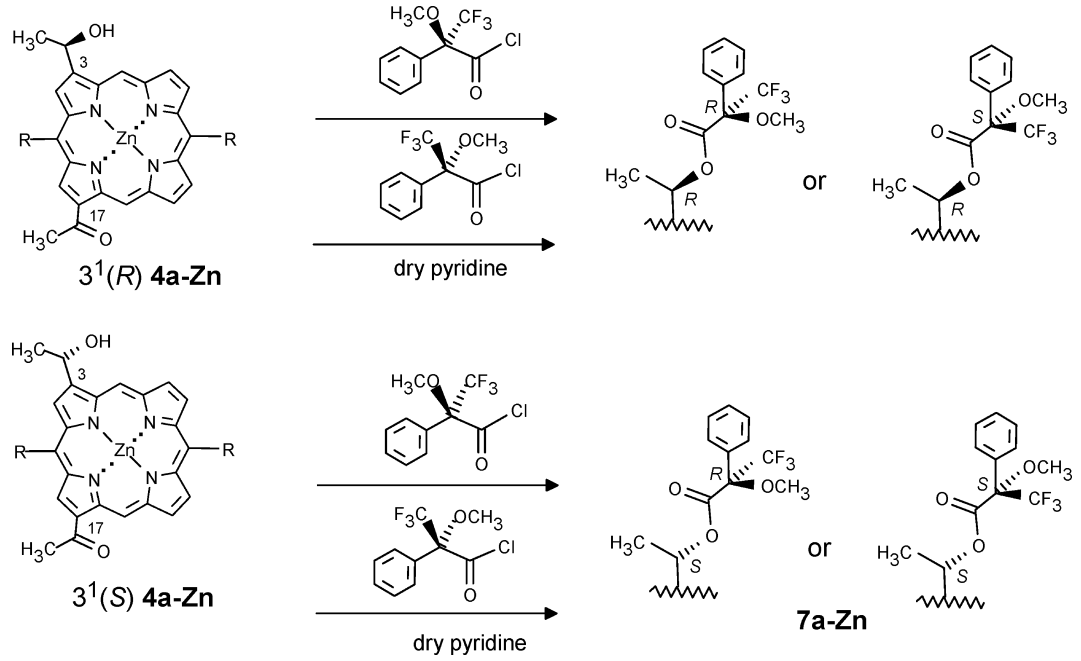

[a] The faster eluting enantiomer of **4a**-**Zn** gave a pair of diastereomeric Mosher's esters, which proved to have the (3^1R)-configuration. The 10,20-substituents R are the 3,5-di-*tert*-butylphenyl group.

Chart 2. Differences ($\Delta\delta \times 1000$) between Chemical Shifts δ (ppm) of Diastereoisomeric MTPA Esters of **7a-Zn**: (a) $\Delta\delta =$ [δ(A2-(*S*)-MTPA) − δ(A2-(*R*)-MTPA] and (b) [δ(B2-(*S*)-MTPA) − δ(B2-(*R*)-MTPA][a]

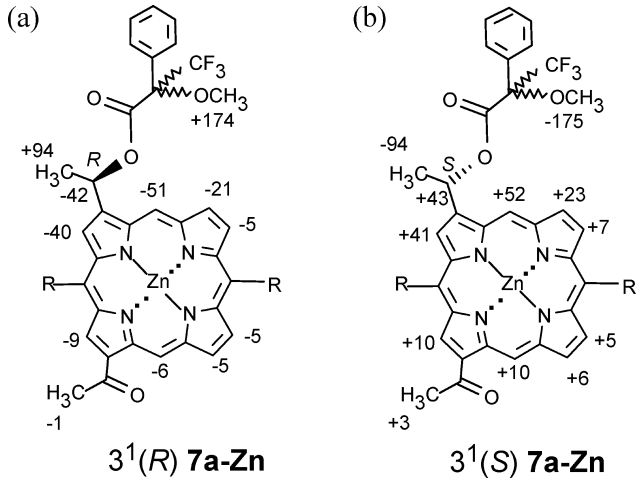

[a] Conclusion: A2, (3^1R)-configuration; B2, (3^1S)-configuration. The 10,20-substituents R are the 3,5-di-*tert*-butylphenyl group.

aggregates,[39] but with considerable broadening, which we ascribe to size heterogeneity. Under the same experimental conditions, the racemates consistently showed increased aggregate maxima (at ca. 450 and 635 nm) for both **4a-Zn** and **5a-Zn** as compared to the resolved enantiomers, which showed more intense Soret bands due to the monomeric forms at ∼422 nm. This supports the fact that a *heterochiral* self-assembly is favored over a *homochiral* one. Another possible explanation could be that the samples, after HPLC separation (which uses 2-propanol) and zinc metalation (which uses methanol), still contain residual amounts of hydroxylic species which hinder self-assembly by coordinating the zinc atoms. We could exclude this hypothesis by preparing the pure enantiomers at a 10 mg scale, followed by washing their dichloromethane solution with brine, which completely removes any alcoholic traces, followed by evaporation of the solvent and prolonged drying under vacuum (10^{-2} bar).

Figures 6 and 7 present the absorption spectra of the racemates and of the separated enantiomers of **4a-Zn** and **5a-Zn**, respectively, after inducing their self-assembly in dry *n*-heptane by dilution of an initial concentrated dichloromethane solution, and after addition of a suprastoichiometric amount of methanol, which leads to a complete disruption of the aggregates due to the formation of the Zn−methanol adducts having the Soret band at ∼434 nm. Also presented in Figures 6 and 7 are the CD spectra of the resolved enantiomers. Figure 6 displays absorption and CD spectra of quiescent solutions of **4a-Zn** aggregated in dry *n*-heptane with a path length of 5 mm.

It has been claimed that a collinear arrangement of the "northern" 3^1-hydroxy substituent with both the central metal atom (Mg or Zn) and the carbonyl substituent situated in the "southern" half of a tetrapyrrolic macrocycle is a *sine-qua-non* condition to observe chlorosomal-type self-assemblies.[40] The results presented here, together with our earlier examples,[10] clearly demonstrate the self-assembly ability of (*rac*)-**4a-Zn**, which does not satisfy this collinearity condition. These apparently contradicting observations can be reconciled by the fact that, in absorption spectra, the aggregate maxima of (*rac*)-**4a-Zn** are less prominent and appear only at higher concentrations than for (*rac*)-**5a-Zn**. Additional examples are presented in the Supporting Information (Figure S9). Consistently, the mono-

(39) (a) Dähne, L. *J. Am. Chem. Soc.* **1995**, *117*, 12855–12860. (b) De Rossi, U.; Dähne, S.; Meskers, C. J.; Dekkers, P. J. M. *Angew. Chem., Int. Ed. Engl.* **1996**, *35*, 760–763. (c) Wang, M.; Silva, G. L.; Armitage, B. A. *J. Am. Chem. Soc.* **2000**, *122*, 9977–9986. (d) Hannah, K. C.; Armitage, B. A. *Acc. Chem. Res.* **2004**, *37*, 845–853.

(40) Tamiaki, H.; Kimura, S.; Kimura, T. *Tetrahedron* **2003**, *59*, 7423–7435.

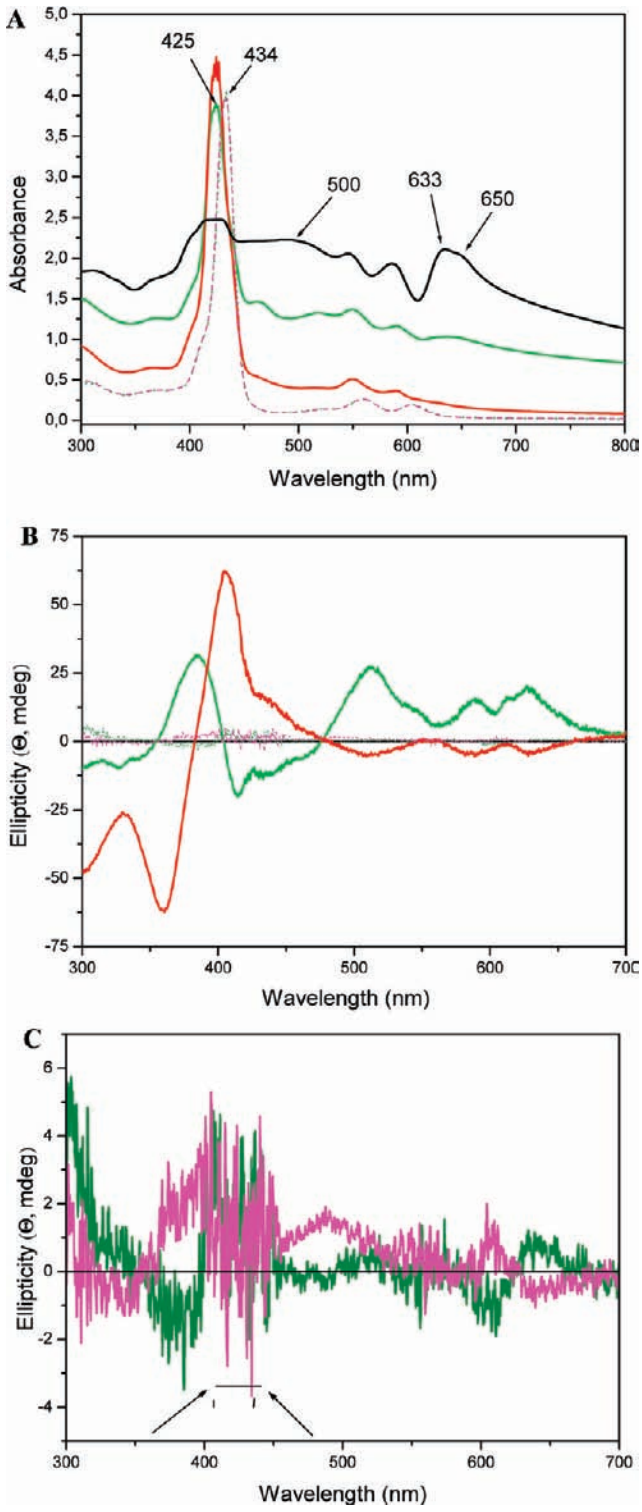

Figure 6. (A) Absorption spectra of **4a-Zn**. Black trace: racemate self-assembled in *n*-heptane; the strong baseline shift is due to light scattering by the nanosized aggregates. Green solid trace: (3^1R) [first-eluted enantiomer on ULMO (*S*,*S*)] self-assembled in *n*-heptane with 5 mm path length. Green dotted trace: (3^1R) after disassembly with MeOH (1 mm path length). Red solid trace: 3^1(*S*) [second-eluted enantiomer] self-assembled in *n*-heptane with 5 mm path length. Magenta dashed trace (superimposed on the green dotted trace): (3^1S) after disassembly with methanol (1 mm path length). (B) Corresponding CD spectra of quiescent solutions in the same 5 mm cuvette. (C) Enlarged portion of the monomeric zinc−methanol adducts after disassembly with methanol, which in part B appear almost superimposed on the zero line (path length 5 mm). Due to the intense absorption by the Soret band, very little light reaches the detector, so the signal in this region, indicated by arrows, is covered by noise.

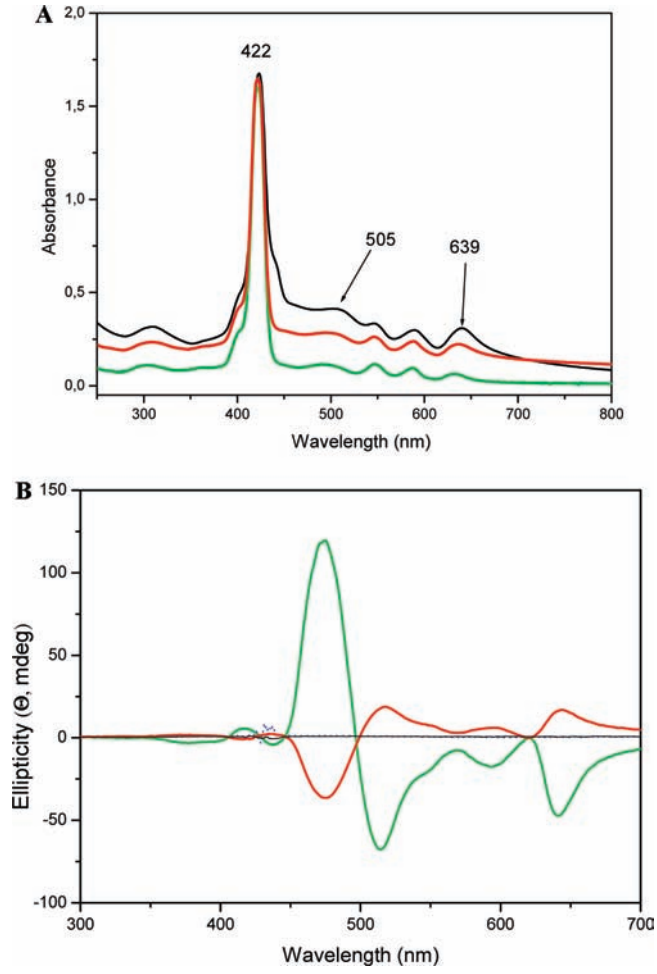

Figure 7. (A) **5a-Zn** self-assembled in quiescent (motionless) *n*-heptane. Black trace: racemate. Green trace: (3^1R) first-eluted enantiomer on ULMO (*S*,*S*). Red trace: (3^1S) second-eluted enantiomer. Note that the racemate has a higher intensity of the aggregate bands at 505 and 639 nm. The baseline shift is due to light scattering by the nanosized aggregates. The red and green traces were scaled to the monomer maximum at 422 nm by multiplying by 1.6 and 3.8, respectively. Upon addition of methanol, the ~505 and ~639 nm maxima vanish completely, along with the baseline shift, due to complete disruption of the aggregates. (B) Corresponding CD spectra measured in the same cuvettes. Note the more intense Cotton effects for the (3^1R)- enantiomer. This is probably due to a higher concentration of oligomeric and higher-aggregated species than for the self-assemblies generated by the (3^1S)-enantiomer. Upon methanol addition, both CD spectra become almost silent. Due to the intense absorption, very little light actually reaches the detector, giving spectra comparable to those for the **4a-Zn** regioisomer after MeOH addition (Figure 6C).

meric Soret bands are much more intense for **4a-Zn** than in the **5a-Zn** isomer. However, in the CD spectra, intense and multiple Cotton effects are encountered after self-assembly for both **4a-Zn** and **5a-Zn**, and these are nearly mirror-images for the respective resolved enantiomers, proving the presence of oligomeric self-assembled species. Upon addition of methanol the CD spectra become practically silent. As previously reported, the chirality of the 3^1-stereocenter induces the supramolecular chirality of these self-assemblies.[10a,b] However, the size heterogeneity and its strong concentration dependence lead to highly variable intensities of the observed Cotton effects. It has been calculated that, for aggregates of chiral chromophores, depending on the aggregate size, even a reversal of the Cotton

effects can be encountered.[41] To summarize, the racemate that self-assembles most readily under the absence of chirality-inducing perturbations gave a silent CD spectrum, while resolved enantiomers gave oligomeric species with approximately mirror-image Cotton effects.

The same behavior could be reproduced with **4b-Zn** and **4c-Zn** (Supporting Information). Suspensions of their self-assemblies are stable in *n*-heptane for much longer periods of time than those of **4a-Zn**. After a few hours, the latter tend to flocculate out of solutions and settle at the bottom of the cuvettes used for measuring optical spectra. Gentle shaking of the cuvette completely disrupts the aggregates, restoring a homogeneous suspension. This property is quite similar to the one encountered previously for *BChl c* aggregates.[7f] For the measurement of absorption, fluorescence, or CD spectra, homogeneous suspensions were used, assuring reproducible results.

Ribó and co-workers have convincingly described that an achiral porphyrin, namely *meso*-tetrakis-4-sulfophenylporphyrin, forms chiral J-aggregates in aqueous solutions and that their helicities are induced by the stirring sense.[42] More recently, Tsuda, Aida, and collaborators have demonstarted an astonishing porphyrin dendrimer that reversibly self-assembles into macroscopic chiral J-aggregates with helicities induced by the vortexing sense.[43] In a preliminary study with enantiopure **4a-Zn**, we observed only negligible effects by reversing the stirring direction of *n*-heptane solutions (Supporting Information, Figures S11 and S12). It may well be that, with longer-chain compounds (e.g., **4b-Zn**, **4c-Zn**, or those obtained by diacylations with other fatty acid chlorides) and with more prolonged and vigorous stirring, such chirality-inducing effects could be possible in nonpolar solvents. These are less viscous than water and thus induce lower shearing forces. In the previous reports by Ribó et al., vigorous vortex stirring was effected for at least 24 h.[41] In our case, 10 min of moderately intense stirring failed to induce the supramolecular chirality of the self-assemblies, which is thus primarily dictated by the 3^1-stereocenter. We explain for **4a-Zn** the absence of a large effect of the stirring sense on the supramolecular chirality by the low content of large, self-assembled species within the enantiopure samples. A prerequisite condition for successful induction of supramolecular chirality by the stirring sense appears to be that a large proportion of higher macroscopic aggregates has to be present after the nucleation step and during the growth phase. Shearing forces can then induce chirality at the macroscopic scale. In the absence of large aggregates, at the nanoscale, no chirality-inducing effects could be observed upon reversing the vortex sense. We compare thus as chirality-inducing effects a substituent effect versus the stirring sense. Preliminary experiments using (*rac*)-**4b-Zn** and, to a lesser extent, (*rac*)-**4a-Zn** show mirror-image CD spectra of films deposited on the cuvette walls upon reversing the vortex sense. However, we suspect that a large contribution to the CD signal comes from linear dichroism (LD). Further experiments with oriented CD and fluorescence detected LD are currently in progress.

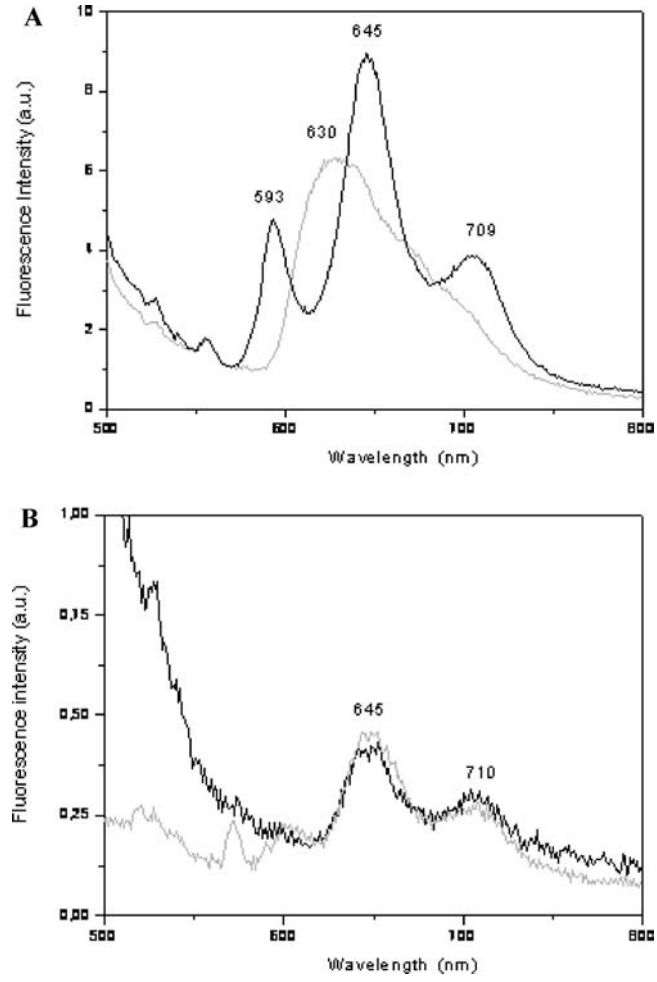

Figure 8. (A) Black trace: solution fluorescence spectrum of aggregates from the racemic **5a-Zn** in dry *n*-heptane recorded in a 1 × 1 cm cuvette with an excitation wavelength of 480 nm. Gray trace: same cuvette after addition of two drops of methanol. (B) Film of ~65 nm thickness deposited on the walls of the same fluorescence cuvette. Excitation wavelength was 480 nm for the black trace and 420 nm for the gray trace.

Typical fluorescence spectra are presented in Figure 8. One can selectively excite the monomeric (in the Soret band at 422 nm) or the self-assembled species (between 450 and 500 nm). After addition of methanol, the Zn−methanol adducts present two intense fluorescence bands, which are more red-shifted (typically at 630 and 700 nm) than those of the monomers accompanying the methanol-free self-assembled species. One can thus easily distinguish between the emission of monomers, either free or coordinated by methanol, and the emission of the self-assemblies, which is quenched by a factor of about 10. Interestingly, if the fluorescence cuvettes have not previously been dried for a longer period (usually overnight) in an oven at >110 °C, the adsorbed water film nucleates the formation on the quartz walls of a thin and ordered aggregate film which is visible to the eye and has a yellow-greenish color. The film fluorescence has a red-shifted shoulder at ~720 nm, as reported before.[44] With randomly oriented chromophores, solid-state fluorescence is usually almost entirely self-quenched. In our case, although the films have at least an order of magnitude less intense fluorescence, this is not entirely quenched due to their orderly supramolecular arrangement. This phenomenon has

(41) (a) Didraga, C.; Klugkist, J. A.; Knoester, J. *J. Phys. Chem. B* **2002**, *106*, 11474–11486. (b) Prokhorenko, V. I.; Steensgaard, D. B.; Holzwarth, A. R. *Biophys. J.* **2003**, *85*, 3173–3186. (c) Pugzlys, A.; Augulis, R.; van Loosdrecht, P. H. M.; Didraga, C.; Malyshev, V. A.; Knoester, J. *J. Phys. Chem. B* **2006**, *110*, 20268–20276.

(42) (a) Ribó, J. M.; Crusats, J.; Sagues, F.; Claret, J. M.; Rubires, R. *Science* **2001**, *292*, 2063–2066. (b) Escudero, C.; Crusats, J.; Diez-Perez, I.; El-Hachemi, Z.; Ribó, J. M. *Angew. Chem., Int. Ed.* **2006**, *45*, 8032–8035. (c) El-Hachemi, Z.; Mancini, G.; Ribó, J. M.; Sorrenti, A. *J. Am. Chem. Soc.* **2008**, *130*, 15176–15184. (d) El-Hachemi, Z.; Arteaga, O.; Canillas, A.; Crusats, J.; Escudero, C.; Kuroda, R.; Harada, T.; Rosa, M.; Ribó, J. M. *Chem.—Eur. J.* **2008**, *14*, 6438–6443.

(43) Tsuda, A.; Alam, Md. A.; Harada, T.; Yamaguchi, T.; Ishii, N.; Aida, T. *Angew. Chem., Int. Ed.* **2008**, *46*, 8198–8202.

been termed "aggregate-induced fluorescence" and has been studied recently by Swager, Park, and co-workers.[45] Figure S12 (Supporting Information) shows the fluorescence spectra of the separated enantiomers of **5a-Zn**, which are quite similar to each other. Again, no major effect could be seen in the fluorescence spectra upon short stirring of the self-assemblies in clockwise or counter-clockwise directions, except for the fact that the aggregate emission was much smaller than for the racemic samples. Fluorescence measurements thus also confirmed that the separated enantiomers do not form as easily and frequently large aggregates as their racemates, as evidenced by the monomer peaks and the fact that the 710−720 nm aggregate peak is much larger for the racemate than for the separated enantiomers.

Scanning Transmission Electron Microscopy (STEM). STEM studies were performed on self-assemblies of (*rac*)-**4a-Zn** and on the respective resolved enantiomers in a similar fashion as described before for **5a-Zn**.[10c] Three conclusions can be derived from these investigations: First, the micrographs (Figure 9 and Supporting Information, Figures S14 and S15) show quite large nanorods, confirming that a collinear arrangement of the 3^1-hydroxyalkyl substituent with the central metal atom and the carbonyl substituent is not mandatory for self-assembly to occur; second, the propensity of the aggregates is much reduced (almost 2 orders of magnitude) in the separated enantiomers as compared to the racemate, proving that the heterochiral self-assembly is thermodynamically favored; and third, all imaged samples, either racemic or enantiopure, show the same fibrillar fine structure at high magnifications, with 1.60 ± 0.05 nm spacings, having the parallel fringes aligned along the long axis of the nanorod. We cannot exclude that the nanorods are initially hollow (i.e., nanotubes or nanotubules) and then, upon drying under ultrahigh vacuum, become collapsed because the tilting of the sample does not change the spacings between fringes. It seems that a rather dense packing of the porphyrins occurs within such rods, which also suffer very easily from damage by the electron beam. To obtain high-resolution images, one has to focus the beam within one range, briefly move the sample, and briskly record the micrograph of a nearby area, which within a few seconds then becomes "burnt out". Fast Fourier transmission of the fringes allows clear diffraction to be obtained (shown in the insets in Figure 9), from which the spacing between the fringes can be calculated.

The resolved enantiomers show mirror-image Cotton effects due to self-aggregation (Figures 6 and 7), but the micrographs present the same lamellar, fine structure without noticeable nanoscopic chirality. We cannot entirely exclude that the imaged nanorods are actually heterochiral assemblies, although the ee's after HPLC resolution were >98%. The paucity of nanorods in the samples of the separated enantiomers could thus be due to the less probable formation of homochiral self-assemblies. A statistical analysis, with samples with various enantiomeric excesses, could shed light on this dilemma, which touches on the long-standing problem related to the obligatory existence of both 3^1-epimers in the chlorosomal *BChl*s.

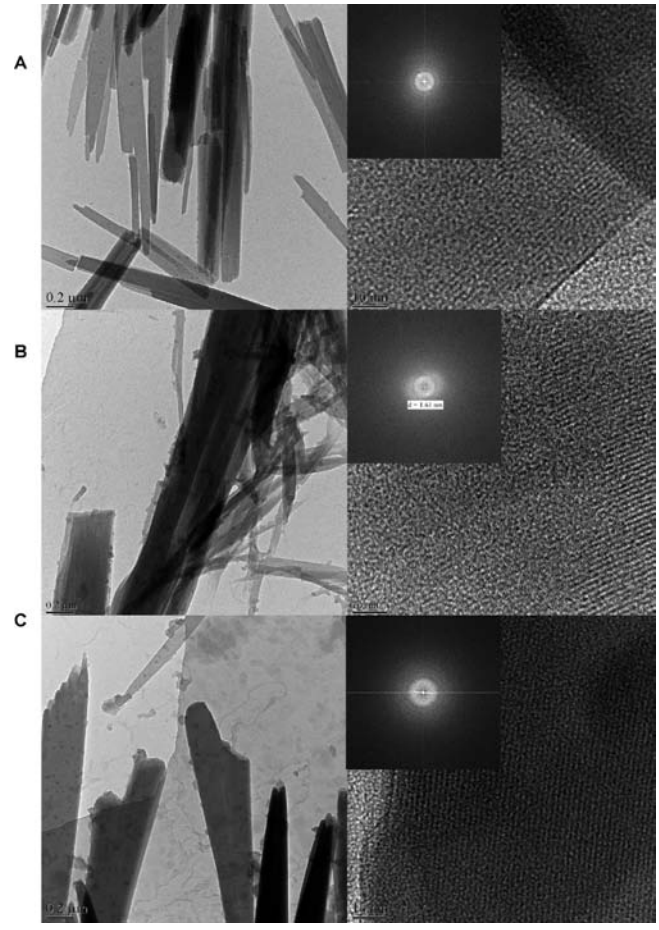

Figure 9. (Left) TEM bright-field micrographs showing assemblies into nanorods of **4a-Zn**: (A) the racemate; (B) the (3^1R)-enantiomer, and (C) the (3^1S)-enantiomer (scale bars are 200 nm). (Right) The corresponding high-resolution images (scale bars are 10 nm) showing striations parallel to the long axis of the nanorod. (Insets) Fast Fourier transform images displaying diffraction spots corresponding to the periodic structure of the molecules. The spacings between fringes were found to be 1.59, 1.61, and 1. 55 nm, respectively.

The observed substantially different rates and propensities for the formation of homochiral and heterochiral aggregates are rather unique and have far-reaching implications. According to the classification proposed by Soloshonok of major intermolecular interactions leading to the self-disproportionation of enantiomers under the conditions of achiral-phase chromatography, preferential formation of heterochiral over homochiral oligomers is considered to be the most rare and has not been observed so far.[46]

Conclusion

The exact nature of the chlorosomal architecture will probably remain elusive in the absence of high-resolution single-crystal

(44) (a) Linke-Schaetzel, M.; Bhise, A. D.; Gliemann, H.; Koch, T.; Schimmel, T.; Balaban, T. S. *Thin Solid Films* **2004**, *451*−*452*, 16–21. (b) Huijser, A.; Marek, P. L.; Savenije, T. J.; Siebbeles, L. D. A.; Scherer, T.; Hauschild, R.; Szmytkowski, J.; Kalt, H.; Hahn, H.; Balaban, T. S. *J. Phys. Chem. C* **2007**, *111*, 11726–11733. (c) Balaban, M. C.; Eichhöfer, A.; Buth, G.; Hauschild, R.; Szmytkowski, R.; Kalt, H.; Balaban, T. S. *J. Phys. Chem. B.* **2008**, *112*, 5512–5521.

(45) (a) Deans, R.; Kim, J.; Machacek, M. R.; Swager, T. M. *J. Am. Chem. Soc.* **2000**, *122*, 8565–8566. (b) Luo, J.; Xie, Z.; Lam, J. W. Y.; Cheng, L.; Chen, H.; Qiu, C.; Kwok, H. S.; Zhan, X.; Liu, X.; Zhu, D.; Tang, B. Z. *Chem. Commun.* **2001**, 1740–1741. (c) An, B.-K.; Kwon, S.-K.; Jung, S.-D.; Park, S. Y. *J. Am. Chem. Soc.* **2002**, *124*, 14410–14415. (d) Bhongale, C. J.; Chang, C.-W.; Diau, E. W.-G.; Hsu, C.-S.; Dong, Y.; Tang, B.-Z. *Chem. Phys. Lett.* **2006**, *419*, 444–449.

(46) (a) Soloshonok, V. A. *Angew. Chem., Int. Ed.* **2006**, *45*, 766–769. (b) Soloshonok, V. A.; Berbasov, D. O. *J. Fluorine Chem.* **2006**, *127*, 597–603. (c) Soloshonok, V. A.; Berbasov, D. O. *Chim. Oggi/Chem. Today* **2006**, *24* (3), 44–47. (d) Soloshonok, V. A.; Ueki, H.; Yasumoto, M.; Mekala, S.; Hirschi, J. S.; Singleton, D. A. *J. Am. Chem. Soc.* **2007**, *129*, 12112–12113.

data. Currently, several controversial models are discussed, such as the lamellar model of Pšenčik et al.[7g] which is based on small-angle X-ray scattering data, and the tubular models based on a combination of solid state NMR-data and electron microscopy images.[7i] Various groups have had repeated attempts to crystallize the chlorosomal *BChl*s, but only nondiffracting material could be isolated after self-assembly.[47] Our studies on synthetic *BChl* mimics have led to self-assemblies that have spectroscopic features similar to those of their respective natural counterparts, and in several of our cases the exact supramolecular architecture could be gleaned by solving crystal structures on the basis of synchrotron X-ray data. It appears possible to infer from our crystal structure(s) the chlorosomal architecture,[10d,f] although the solubility-inducing groups, which are involved only in recessive weak supramolecular interactions, are quite different from the ones found in *BChl*s. In the present study, after optimizing regioselective diacylations of porphyrins and HPLC methods to obtain enantiopure *BChl* mimics, we have studied their ability to self-assemble. The spectroscopic and nanoscopic investigations point toward a more favored heterochiral self-assembly process in the case of only one stereogenic center present on the porphyrin periphery as 3-hydroxyalkyl groups. We infer from this that the natural chlorosomal *BChl*s use the same mechanism for self-assembly, which leads to larger structures if both 3^1-epimers are present. This correlates well with the observed up-regulation of the biosyntheses under low-light illumination conditions of the less abundant (3^1S)-epimers.[14] The bias toward a less favored self-assembly with epimerically enriched (3^1R)-homologues could provide a way to assemble smaller chlorosomes and thus regulate the light-harvesting ability when sufficient quantities of photons are available. The chirality of the 3^1-stereocenter appears thus to play a key role in regulating a physical property, namely the antenna function. Ongoing studies in our laboratories should shed light on this long-standing problem, which has evolutionary implications, as well as allowing the design of efficient artificial light-harvesting systems.

(47) (a) Fajer, J., and Smith, K. M., personal communications. (b) Over a period of 15 years, we have been unable to grow single crystals from a variety of *BChl c* homologues.

Acknowledgment. We gratefully acknowledge Dr. T. Bruhn and Dr. M. Reichert (University of Würzburg) for their computational contributions. We thank the Deutsche Forschungsgemeinschaft (DFG) for partial support in Karlsruhe through the Center for Functional Nanostructures (CFN) through projects C3.2 and C3.5 "Energy Transfer Studies of Artificial Mimics of Natural Light Harvesting Molecules". Collaborative work between Karlsruhe and Marseille was supported by the CNRS through PICS no. 3777. This work in Japan was partially supported by Grants-in-Aid for Scientific Research (B) (No. 19350088, to H.T.) from the Japanese Society for the Promotion of Science (JSPS) and for Young Scientists (B) (no. 19750148, to T.M.) from the Ministry of Education, Culture, Sports, Science and Technology. This work in Würzburg was supported by the Degussa Stiftung and the Studienstiftung des deutschen Volkes e.V. (fellowships to D.C.G.G.). We dedicate this work to Prof. Jean-Marie Lehn on the occasion of his 70th birthday.

Supporting Information Available: Detailed experimental procedures and additional illustrative spectral data. This material is available free of charge via the Internet at http://pubs.acs.org.

JA905628H